electronic reprint

CRYSTALLOGRAPHIC COMMUNICATIONS

ISSN: 2056-9890
journals.iucr.org/e

Synthesis and crystal structure of 1,3-bis(4-hydroxyphenyl)-1*H*-imidazol-3-ium chloride

R. Tyler Mertens, Sean R. Parkin and Samuel G. Awuah

Acta Cryst. (2019). E**75**, 1311–1315

Acta Cryst E CRYSTALLOGRAPHIC COMMUNICATIONS

ISSN 2056-9890

Synthesis and crystal structure of 1,3-bis(4-hydroxyphenyl)-1*H*-imidazol-3-ium chloride

R. Tyler Mertens, Sean R. Parkin and Samuel G. Awuah*

Department of Chemistry, University of Kentucky, Lexington, Kentucky 40506, USA. *Correspondence e-mail: awuah@uky.edu

Received 11 July 2019
Accepted 8 August 2019

Edited by H. Stoeckli-Evans, University of Neuchâtel, Switzerland

Keywords: crystal structure; imidazolium salt; *N*-heterocyclic carbene; hydrogen bonding; Hirshfeld surface.

CCDC reference: 1946122

Supporting information: this article has supporting information at journals.iucr.org/e

Imidazolium salts are common building blocks for functional materials and in the synthesis of N-heterocyclic carbene (NHC) as σ-donor ligands for stable metal complexes. The title salt, 1,3-bis(4-hydroxyphenyl)-1*H*-imidazol-3-ium chloride (IOH·Cl), $C_{15}H_{13}N_2O_2^+\cdot Cl^-$, is a new imidazolium salt with a hydroxy functionality. The synthesis of IOH·Cl was achieved in high yield *via* a two-step procedure involving a diazabutadiene precursor followed by ring closure using trimethylchlorosilane and paraformaldehyde. The structure of IOH·Cl consists of a central planar imidazolium ring (r.m.s. deviation = 0.0015 Å), with out-of-plane phenolic side arms. The dihedral angles between the 4-hydroxyphenyl substituents and the imidazole ring are 55.27 (7) and 48.85 (11)°. In the crystal, O—H···Cl hydrogen bonds connect the distal hydroxy groups and Cl^- anions in adjacent asymmetric units, one related by inversion ($-x+1, -y+1, -z+1$) and one by the *n*-glide ($x-\frac{1}{2}, -y+\frac{1}{2}, z-\frac{1}{2}$), with donor–acceptor distances of 2.977 (2) and 3.0130 (18) Å, respectively. The phenolic rings are each π–π stacked with their respective inversion-related [($-x+1, -y+1, -z+1$) and ($-x, -y+1, -z+1$)] counterparts, with interplanar distances of 3.560 (3) and 3.778 (3) Å. The only other noteworthy intermolecular interaction is an O···O (not hydrogen bonded) close contact of 2.999 (3) Å between crystallographically different hydroxy O atoms on translationally adjacent molecules ($x+1, y, x+1$).

1. Chemical context

N-Heterocyclic carbenes (NHCs) represent a versatile class of ligand systems for metal-center activation or stabilization in modern organic synthesis (Arduengo *et al.*, 1999; Benhamou *et al.*, 2011). Chemically, carbenes are nucleophilic 'phosphine mimics' that are high in the order of the Tolman electronic and steric parameter scales, which influences their reactivity. Metal complexes bearing NHC ligands are found in many catalytic reactions (Flanigan *et al.*, 2015; Hopkinson *et al.*, 2014; Huynh, 2018; Marion & Nolan, 2008; Scholl *et al.*, 1999; Velazquez & Verpoort, 2012; Wang *et al.*, 2018), and recently have shown promise as cytotoxic agents (Garrison & Youngs, 2005; Lam *et al.*, 2018; Liu & Gust, 2013; Mora *et al.*, 2019; Riener *et al.*, 2014; Zou *et al.*, 2018). Imidazolium salts, which are simple salts of the free carbene, are commonly used in many systems in preference to their free carbene counterparts due to their high stability. Unlike the free carbenes, which readily react with water or oxygen (Alder *et al.*, 1995), imidazolium salts are indefinitely stable. Use of the imidazolium salt does not require Schlenk techniques and the corresponding 'free' carbene can be prepared *in situ via* deprotonation with a strong base (*e.g.* NaO^{t}Bu and NaH) (Arduengo *et al.*, 1991; McGuinness *et al.*, 2001; Hauwert *et al.*, 2008; Voutchkova *et al.*, 2005). Expanding the functional diversity of NHC ligands

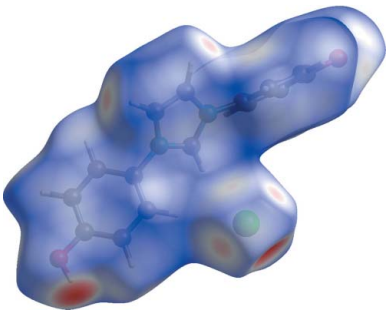

Table 1
Hydrogen-bond geometry (Å, °).

D—H···A	D—H	H···A	D···A	D—H···A
O1—H1O···Cl1^{i}	0.93 (3)	2.06 (3)	2.975 (2)	169 (3)
O2—H2O···Cl1^{ii}	0.89 (3)	2.13 (3)	3.0118 (19)	171 (3)
C1—H1···O1^{i}	0.95	2.45	3.280 (3)	145
C1—H1···O2^{iii}	0.95	2.51	3.271 (3)	137
C2—H2···Cl1^{iv}	0.95	2.80	3.647 (3)	150
C3—H3···Cl1^{v}	0.95	2.74	3.655 (3)	163

Symmetry codes: (i) $-x+1, -y+1, -z+1$; (ii) $x-\frac{1}{2}, -y+\frac{1}{2}, z-\frac{1}{2}$; (iii) $-x, -y+1, -z$; (iv) $-x, -y+1, -z+1$; (v) $-x-\frac{1}{2}, y+\frac{1}{2}, -z+\frac{1}{2}$.

will broaden their utility. The synthesis of the novel imidazolium salt in this report offers a unique extension of previously reported imidazolium salts through the addition of phenolic groups, herein referred to as IOH·Cl, for functionalization (see Scheme). The hydroxyl functional group presents the possibility of tethering other chemical groups for varied applications, including catalysis, materials, and biomedicine. The synthesis of IOH·Cl (Fig. 1) does not require Schlenk techniques and the product is isolated as an air-stable solid that can be stored indefinitely without decomposition. The synthesis is part of a study to develop reaction methods for C—N bond formation from high-oxidation-state transition metals.

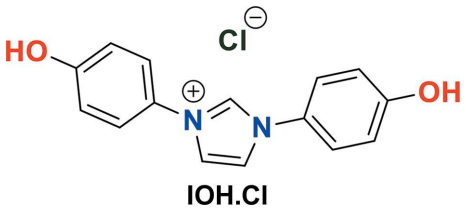

2. Structural commentary

In the structure of IOH·Cl (Fig. 2), there are no unusual bond lengths or angles. The organic cation consists of a central planar imidazolium ring (r.m.s. deviation = 0.0015 Å), with *para*-phenol substituents (C4–C9/O1 and C10–C16/O2) bonded to the imidazolium N atoms [N1—C4 = 1.442 (3) Å and N2—C10 = 1.441 (3) Å]. The phenol groups are out-of-plane, forming dihedral angles with the imidazolium ring of 55.27 (7) and 48.85 (11)° for rings C4–C9 and C10–C15, respectively. The hydroxy H-atom coordinates were refined freely and are slightly out-of-plane of their respective phenolic groups; the torsion angles are 9.1 (19)° for C6—C7—O1—H1O and 11 (2)° for C12—C13—O2—H2O.

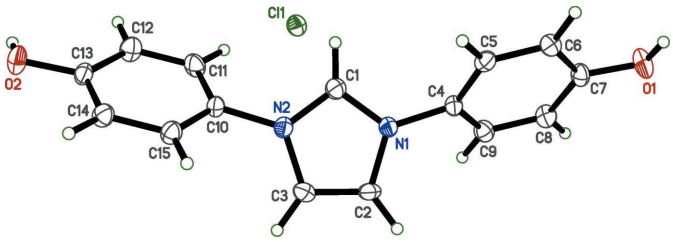

Figure 2
The molecular structure of IOH·Cl, with displacement ellipsoids drawn at the 50% probability level.

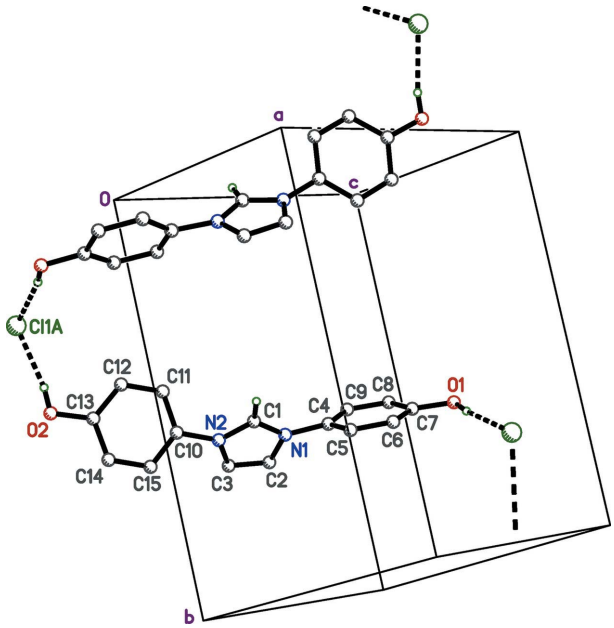

Figure 3
A plot of the O—H···Cl hydrogen bonds in crystals of IOH·Cl. These interactions, drawn as dashed solid lines, link molecules into head-to-tail zigzag chains that extend parallel to the *b* axis. The unlabelled molecule is related to its labelled counterpart by the crystallographic 2_1 screw axis $(-x+\frac{1}{2}, y-\frac{1}{2}, -z+\frac{1}{2})$.

3. Supramolecular features

The most prominent intermolecular interactions in the crystals of IOH·Cl are O—H···Cl hydrogen bonds. These link the Cl^- anion at (x, y, z) to two different IOH·Cl molecules, one related by inversion and the other by the *n*-glide. These hydrogen bonds, *viz.* O1^{i}—H1O^{i}···Cl1 and O2^{ii}—H2O^{ii}—Cl1 [symmetry codes: (i) $-x+1, -y+1, -z+1$; (ii) $x+\frac{1}{2}, -y+\frac{1}{2}, z+\frac{1}{2}$; Fig. 3 and Table 1], have donor–acceptor distances of 2.975 (2) and 3.012 (2) Å, respectively. Weaker bifurcated C—

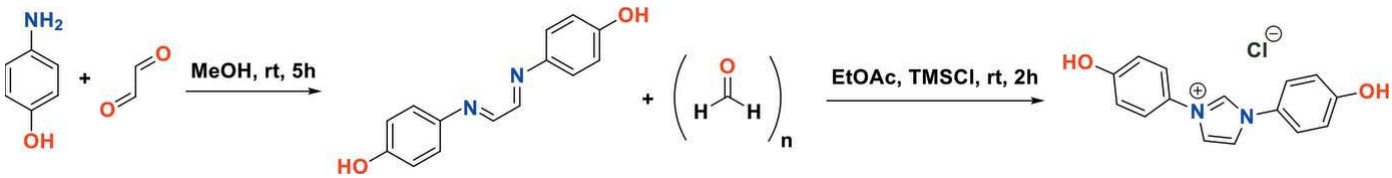

Figure 1
Synthesis of IOH·Cl.

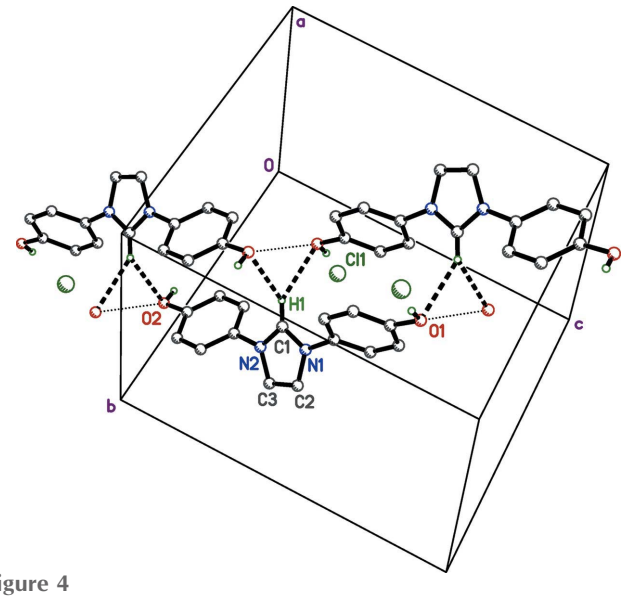

Figure 4
A plot showing the bifurcated C—H···O interactions (dashed solid lines) and O···O close contacts (dotted lines) in crystalline IOH·Cl. The unlabelled molecules are related to the partially labelled molecule by inversion [upper left: $(-x, -y + 1, -z)$; upper right: $(-x + 1, -y + 1, -z + 1)$].

H···O interactions occur between imidazole ring atoms (C1—H1) and hydroxy O atoms ($O1^{i}$ and $O2^{iii}$) on molecules related by different inversion centres. These same hydroxy O atoms are in close contact with each other, *i.e.* $O1^{i}\cdots O2^{iii}$ = 2.999 (3) Å [symmetry codes: (i) $-x + 1, -y + 1, -z + 1$; (iii) $-x, -y + 1, -z$; Fig. 4]. In addition to hydrogen bonding, there are offset π–π stacking interactions (Fig. 5). The perpendicular stacking distance between the C4–C9 benzene ring and an inversion-related equivalent at $(-x + 1, -y + 1, -z + 1)$ is 3.560 (3) Å. The overlap of the C10–C15 benzene ring C10–C15 with an inversion-related equivalent at $(-x, -y + 1, -z)$ is weaker, giving a perpendicular stacking distance of 3.777 (3) Å. All hydrogen-bond interactions are readily apparent in the Hirshfeld surface and fingerprint plots (McKinnon *et al.*, 2007; Turner *et al.*, 2017; Tan *et al.*, 2019). In Fig. 6(*a*), the prominent deep-red ellipse-shaped regions represent the O—H···Cl hydrogen bonds, while the faint-red regions represent the bifurcated C—H···O interactions (Table 1). Short contacts between the imidazole ring and inversion [C2—H2···Cl^{iv}; symmetry code: (iv) $-x, -y + 1, -z + 1$] and 2_1-screw [C3—H3···Cl^{v}; symmetry code: (v) $-x - \frac{1}{2}, y + \frac{1}{2}, -z + \frac{1}{2}$] related anions are also apparent (Fig. 6*b* and Table 1). Hirshfeld-surface 'fingerprint plots' (Figs. 7*a–f*) quantify the majority of intermolecular contacts as H···H (36.2%; Fig. 7*b*) and C···H (21.7%; Fig. 7*c*). In these diagrams, the O—H···Cl hydrogen bonds are indicated by sharp diagonal jutting spikes (Fig. 7*d*), while C—H···O interactions give less-pronounced spikes (Fig. 7*e*). C···C contacts, which are all as a result of π–π stacking, account for 6.6% of the intermolecular contacts (Fig. 7*f*).

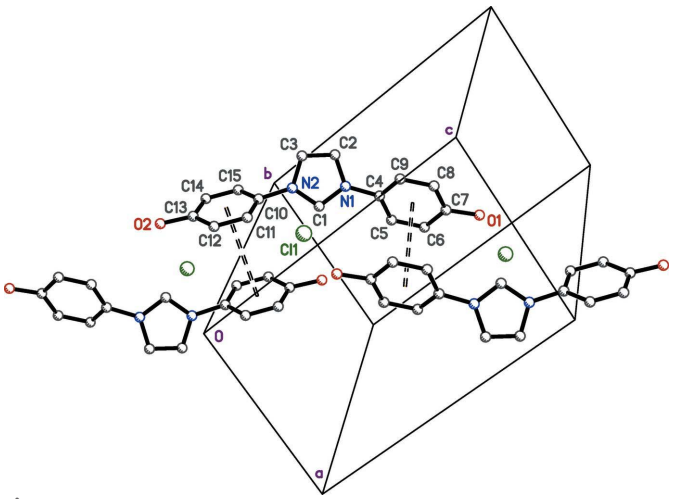

Figure 5
A plot highlighting the π–π stacking (open dashed lines) of benzene rings in crystals of IOH·Cl. Unlabelled molecules are related to the labelled molecule by inversion [lower right: $(-x + 1, -y + 1, -z + 1)$; lower left: $(-x, -y + 1, -z)$].

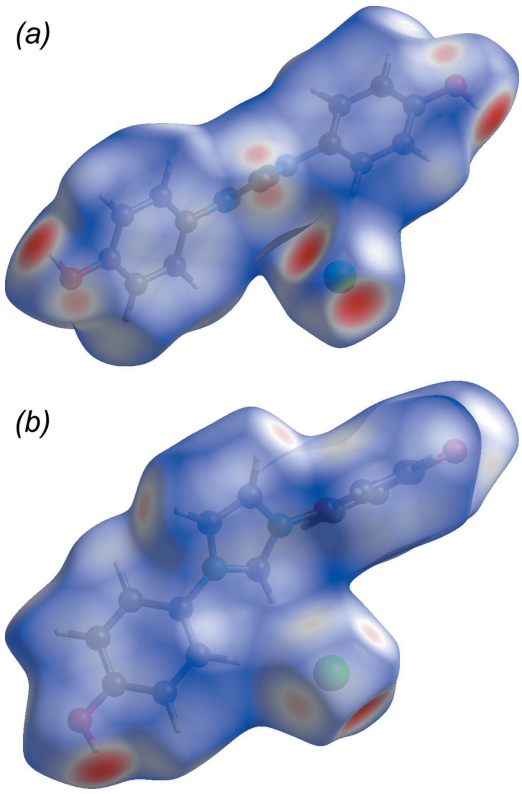

Figure 6
Two views of the normalized contact distances, d_{norm}, mapped onto the Hirshfeld surface of IOH·Cl. In (*a*), the larger red regions correspond to the O—H···Cl hydrogen bonds, while the smaller pink regions correspond to the C—H···O bifurcated weak hydrogen bonds. In (*b*), the faint-pink regions in the upper middle of the diagram correspond to close contacts between imidazole-ring C—H groups and Cl^{-} anions.

4. Database survey

A search of the Cambridge Structural Database (CSD; Version 5.40, November 2018; Groom *et al.*, 2016) on the three-ring fragment of the title compound yielded over 600

hits, ranging from similar simple salts to metal complexes containing analogous NHC frameworks. A search with H atoms bonded to the three carbons of the imidazole ring gave 180 hits. Of these, 28 had mesityl substituents, including IHOQUS (IMes·Cl; Lorber & Vendier, 2009) and GAKCAZ (IMes·BF_4; Bethel *et al.*, 2016), and 62 had 2,6-diisopropylphenyl groups, including KIDKUG (IPr·ClO_4; Minaker *et al.*, 2018), OHURIU (IPr·PF_6; Rheingold *et al.*, 2015), TAXLOW (IPr·SiF_5; Ališ *et al.*, 2017), and XANPEJ (IPr·I; Solovyev *et al.*, 2010). Structures most similar to IOH·Cl in the present work include the commonly used IMes·Cl (IHOQUS) and IPr·ClO_4 (KIDKUG), and the unsubstituted phenyl analog IPh·ClO_4 (DPIMPC; Luger & Ruban, 1975). A more restrictive search with only *para* substitution allowed on the phenyl rings gave 47 hits, of which 44 were carboxylates that formed extended polymeric structures with metal-containing species. The remaining three, BOGVAV (Wan *et al.*, 2008), TUPYAF (Garden *et al.*, 2010), and DAQKOW (Suisse *et al.*, 2005), have –OMe, –Br, and $–OC_{12}H_{25}$ groups at the *para* position. One other structure with comparative functionalization is LEBMUC (Schedler *et al.*, 2012), which bears bis-methoxy groups at the *ortho*-phenyl-ring positions.

5. Synthesis and crystallization

The overall reaction for the synthesis of the title compound is depicted in Fig. 1. Step 1, *Synthesis of the precursor N,N′-bis(4-hydroxyphenyl)-1,4-diazabutadiene (1)*: to a round-bottomed flask charged with 15 ml of methanol, 4-phenolaniline (813 mg, 7 mmol) was added and stirred until fully dissolved. Glyoxal (174 mg, 3 mmol) was added to the reaction solution with stirring. Upon addition of glyoxal solution, 40 wt.% in H_2O, a brown precipitate formed and the solution turned orange. The reaction was further stirred at room temperature for 5 h and the solid was vacuum filtered and washed with cold methanol (612 mg, 85% yield). Step 2, *Synthesis of IOH·Cl*:

Table 2
Experimental details.

Crystal data	
Chemical formula	$C_{15}H_{13}N_2O_2^+\cdot Cl^-$
M_r	288.72
Crystal system, space group	Monoclinic, $P2_1/n$
Temperature (K)	90
a, b, c (Å)	8.1752 (6), 13.2684 (8), 12.7391 (10)
β (°)	100.105 (3)
V (Å^3)	1360.40 (17)
Z	4
Radiation type	Mo $K\alpha$
μ (mm^{-1})	0.28
Crystal size (mm)	0.24 × 0.03 × 0.03
Data collection	
Diffractometer	Bruker D8 Venture dual source
Absorption correction	Multi-scan (*SADABS*; Krause *et al.*, 2015)
T_{min}, T_{max}	0.821, 0.928
No. of measured, independent and observed [$I > 2\sigma(I)$] reflections	14925, 3109, 1869
R_{int}	0.103
(sin $\theta/\lambda)_{max}$ (Å^{-1})	0.649
Refinement	
$R[F^2 > 2\sigma(F^2)]$, $wR(F^2)$, S	0.049, 0.083, 1.01
No. of reflections	3109
No. of parameters	187
H-atom treatment	H atoms treated by a mixture of independent and constrained refinement
$\Delta\rho_{max}$, $\Delta\rho_{min}$ (e Å^{-3})	0.34, −0.32

Computer programs: *APEX3* (Bruker, 2016), *SHELXT* (Sheldrick, 2015*a*), *XP* in *SHELXTL* (Sheldrick, 2008), *SHELXL2018* (Sheldrick, 2015*b*) and *CIFFIX* (Parkin, 2013).

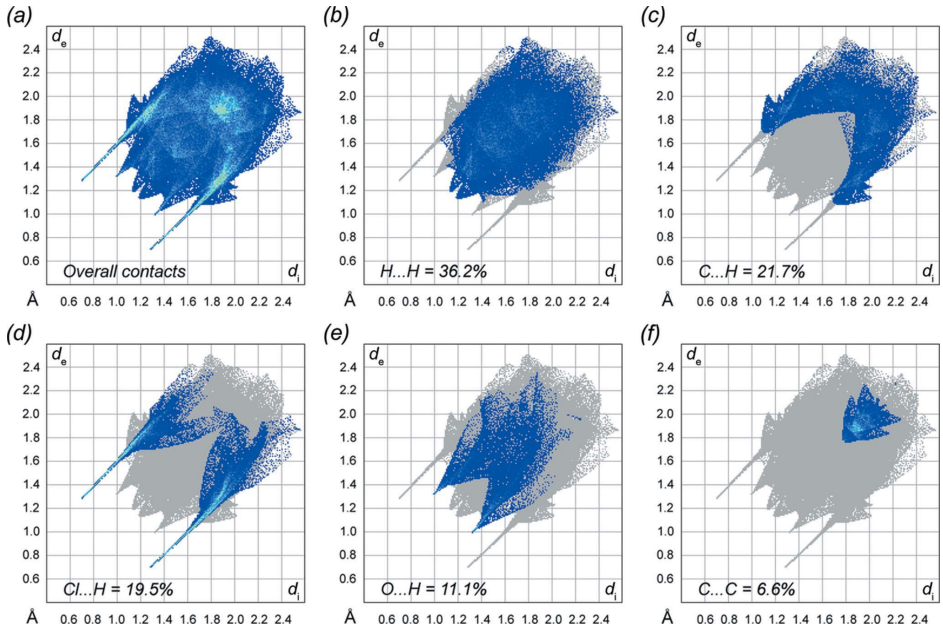

Figure 7
(*a*) The full 2D (two-dimensional) fingerprint plot for IOH·Cl, along with separate plots highlighting the five most important and abundant specific contacts: (*b*) H···H, (*c*) C···H, (*d*) Cl···H, (*e*) O···H, and (*f*) C···C.

ethyl acetate (10 ml) was pre-heated to 343 K. To the hot solution was added (1) (200 mg, 1.2 mmol) and paraformaldehyde (36 mg, 1.2 mmol). The reaction mixture was stirred until all of the paraformaldehyde had dissolved. To this was added a solution of trimethylchlorosilane (TMSCl) (0.2 ml, 130 mg, 1.2 mmol) in ethyl acetate (0.15 ml) dropwise over 5 min while stirring. The solution was stirred for 2 h and then placed in a refrigerator (275 K) overnight. The precipitate was collected by vacuum filtration and washed with cold ethyl acetate and ether until the filtrate was colorless, yielding a dark-orange solid (yield 208 mg, 60%). Crystals were grown by slow evaporation of a concentrated solution in acetone.

6. Refinement

Crystal data, data collection, and structure refinement details are given in Table 2. All H atoms were found in difference Fourier maps. Hydroxy H-atom coordinates were refined freely, with $U_{iso}(H) = 1.5U_{eq}(O)$. Carbon-bound H atoms were included in calculated positions and refined using a standard riding model, with C—H = 0.95 Å and $U_{iso}(H) = 1.2U_{eq}(C)$. Refinement progress was checked using an *R*-tensor (Parkin, 2000), *PLATON* (Spek, 2009), and *checkCIF* (https://checkcif.iucr.org/).

Funding information

Funding for this research was provided by: National Science Foundation (MRI CHE1625732), and by the University of Kentucky.

References

Alder, R. W., Allen, P. R. & Williams, S. J. (1995). *J. Chem. Soc. Chem. Commun.* pp. 1267–1268.
Ališ, B., Tramšek, M., Kokalj, A. & Tavčar, G. (2017). *Inorg. Chem.* **56**, 10070–10077.
Arduengo, A. J., Harlow, R. L. & Kline, M. (1991). *J. Am. Chem. Soc.* **113**, 2801–2801.
Arduengo, A. J., Krafczyk, R., Schmutzler, R., Craig, H. A., Goerlich, J. R., Marshall, W. J. & Unverzagt, M. (1999). *Tetrahedron*, **55**, 14523–14534.
Benhamou, L., Chardon, E., Lavigne, G., Bellemin-Laponnaz, S. & César, V. (2011). *Chem. Rev.* **111**, 2705–2733.
Bethel, R., Denny, J. A. & Darensbourg, M. Y. (2016). *CSD Private communication*. CCDC 1450616. CCDC, Cambridge, England.
Bruker (2016). *APEX3*. Bruker AXS Inc., Madison, Wisconsin, USA.
Flanigan, D. M., Romanov-Michailidis, F., White, N. A. & Rovis, T. (2015). *Chem. Rev.* **115**, 9307–9387.
Garden, S. J., Gama, P. E., Tiekink, E. R. T., Wardell, J. L., Wardell, S. M. S. V. & Howie, R. A. (2010). *Acta Cryst.* E**66**, o1438–o1439.
Garrison, J. C. & Youngs, W. J. (2005). *Chem. Rev.* **105**, 3978–4008.
Hauwert, P., Maestri, G., Sprengers, J. W., Catellani, M. & Elsevier, C. J. (2008). *Angew. Chem. Int. Ed.* **47**, 3223–3226.
Hopkinson, M. N., Richter, C., Schedler, M. & Glorius, F. (2014). *Nature*, **510**, 485–496.
Huynh, H. V. (2018). *Chem. Rev.* **118**, 9457–9492.
Krause, L., Herbst-Irmer, R., Sheldrick, G. M. & Stalke, D. (2015). *J. Appl. Cryst.* **48**, 3–10.
Lam, N. Y. S., Truong, D., Burmeister, H., Babak, M. V., Holtkamp, H. U., Movassaghi, S., Ayine-Tora, D. M., Zafar, A., Kubanik, M., Oehninger, L., Söhnel, T., Reynisson, J., Jamieson, S. M. F., Gaiddon, C., Ott, I. & Hartinger, C. G. (2018). *Inorg. Chem.* **57**, 14427–14434.
Liu, W. & Gust, R. (2013). *Chem. Soc. Rev.* **42**, 755–773.
Lorber, C. & Vendier, L. (2009). *Dalton Trans.* pp. 6972–6984.
Luger, P. & Ruban, G. (1975). *Z. Kristallogr.* **142**, 177–185.
Marion, N. & Nolan, S. P. (2008). *Chem. Soc. Rev.* **37**, 1776–1782.
McGuinness, D. S., Saendig, N., Yates, B. F. & Cavell, K. J. (2001). *J. Am. Chem. Soc.* **123**, 4029–4040.
McKinnon, J. J., Jayatilaka, D. & Spackman, M. A. (2007). *Chem. Commun.* pp. 3814–3816.
Minaker, S. A., Wang, R. & Aquino, M. A. S. (2018). *IUCrData*, **3**, x180516.
Mora, M., Gimeno, M. C. & Visbal, R. (2019). *Chem. Soc. Rev.* **48**, 447–462.
Parkin, S. (2000). *Acta Cryst.* A**56**, 157–162.
Parkin, S. (2013). *CIFFIX*, https://xray.uky.edu/Resources/scripts/ciffix.
Rheingold, A. L., Wang, G. & Glueck, D. S. (2015). CCDC 1408942. *CSD Private communication*. CCDC, Cambridge, England.
Riener, K., Haslinger, S., Raba, A., Högerl, M. P., Cokoja, M., Herrmann, W. A. & Kühn, F. E. (2014). *Chem. Rev.* **114**, 5215–5272.
Schedler, M., Fröhlich, R., Daniliuc, C. G. & Glorius, F. (2012). *Eur. J. Org. Chem.* **2012**, 4164–4171.
Scholl, M., Ding, S., Lee, C. W. & Grubbs, R. H. (1999). *Org. Lett.* **1**, 953–956.
Sheldrick, G. M. (2008). *Acta Cryst.* A**64**, 112–122.
Sheldrick, G. M. (2015*a*). *Acta Cryst.* A**71**, 3–8.
Sheldrick, G. M. (2015*b*). *Acta Cryst.* C**71**, 3–8.
Solovyev, A., Chu, Q., Geib, S. J., Fensterbank, L., Malacria, M., Lacôte, E. & Curran, D. P. (2010). *J. Am. Chem. Soc.* **132**, 15072–15080.
Spek, A. L. (2009). *Acta Cryst.* D**65**, 148–155.
Suisse, J.-M., Bellemin-Laponnaz, S., Douce, L., Maisse-François, A. & Welter, R. (2005). *Tetrahedron Lett.* **46**, 4303–4305.
Tan, S. L., Jotani, M. M. & Tiekink, E. R. T. (2019). *Acta Cryst.* E**75**, 308–318.
Turner, M. J., Mckinnon, J. J., Wolff, S. K., Grimwood, D. J., Spackman, P. R., Jayatilaka, D. & Spackman, M. A. (2017). *CrystalExplorer17*. The University of Western Australia.
Velazquez, H. D. & Verpoort, F. (2012). *Chem. Soc. Rev.* **41**, 7032–7060.
Voutchkova, A. M., Appelhans, L. N., Chianese, A. R. & Crabtree, R. H. (2005). *J. Am. Chem. Soc.* **127**, 17624–17625.
Wan, Y., Xin, H., Chen, X., Xu, H. & Wu, H. (2008). *Acta Cryst.* E**64**, o2159.
Wang, W., Cui, L., Sun, P., Shi, L., Yue, C. & Li, F. (2018). *Chem. Rev.* **118**, 9843–9929.
Zou, T., Lok, C.-N., Wan, P.-K., Zhang, Z.-F., Fung, S.-K. & Che, C.-M. (2018). *Curr. Opin. Chem. Biol.* **43**, 30–36.

supporting information

Acta Cryst. (2019). E**75**, 1311-1315 [https://doi.org/10.1107/S2056989019011058]

Synthesis and crystal structure of 1,3-bis(4-hydroxyphenyl)-1*H*-imidazol-3-ium chloride

R. Tyler Mertens, Sean R. Parkin and Samuel G. Awuah

Computing details

Data collection: *APEX3* (Bruker, 2016); cell refinement: *APEX3* (Bruker, 2016); data reduction: *APEX3* (Bruker, 2016); program(s) used to solve structure: *SHELXT* (Sheldrick, 2015a); program(s) used to refine structure: *SHELXL2018* (Sheldrick, 2015b); molecular graphics: *XP* in *SHELXTL* (Sheldrick, 2008); software used to prepare material for publication: *SHELXL2018* (Sheldrick, 2015b) and *CIFFIX* (Parkin, 2013).

1,3-Bis(4-hydroxyphenyl)-1*H*-imidazol-3-ium chloride

Crystal data

$C_{15}H_{13}N_2O_2^+ \cdot Cl^-$
$M_r = 288.72$
Monoclinic, $P2_1/n$
$a = 8.1752$ (6) Å
$b = 13.2684$ (8) Å
$c = 12.7391$ (10) Å
$\beta = 100.105$ (3)°
$V = 1360.40$ (17) Å^3
$Z = 4$
$F(000) = 600$
$D_x = 1.410$ Mg m^{-3}
Mo $K\alpha$ radiation, $\lambda = 0.71073$ Å
Cell parameters from 1847 reflections
$\theta = 3.2$–25.1°
$\mu = 0.28$ mm^{-1}
$T = 90$ K
Needle, pale yellow
0.24 × 0.03 × 0.03 mm

Data collection

Bruker D8 Venture dual source diffractometer
Radiation source: microsource
Detector resolution: 7.41 pixels mm^{-1}
φ and ω scans
Absorption correction: multi-scan (*SADABS*; Krause *et al.*, 2015)
$T_{min} = 0.821$, $T_{max} = 0.928$
14925 measured reflections
3109 independent reflections
1869 reflections with $I > 2\sigma(I)$
$R_{int} = 0.103$
$\theta_{max} = 27.5°$, $\theta_{min} = 2.2°$
$h = -10 \rightarrow 10$
$k = -12 \rightarrow 17$
$l = -16 \rightarrow 16$

Refinement

Refinement on F^2
Least-squares matrix: full
$R[F^2 > 2\sigma(F^2)] = 0.049$
$wR(F^2) = 0.083$
$S = 1.01$
3109 reflections
187 parameters
0 restraints
Primary atom site location: structure-invariant direct methods
Secondary atom site location: difference Fourier map
Hydrogen site location: mixed
H atoms treated by a mixture of independent and constrained refinement
$w = 1/[\sigma^2(F_o^2) + 0.9975P]$ where $P = (F_o^2 + 2F_c^2)/3$
$(\Delta/\sigma)_{max} < 0.001$
$\Delta\rho_{max} = 0.34$ e Å^{-3}
$\Delta\rho_{min} = -0.32$ e Å^{-3}

Special details

Experimental. The crystal was mounted using polyisobutene oil on the tip of a fine glass fibre, which was fastened in a copper mounting pin with electrical solder. It was placed directly into the cold gas stream of a liquid-nitrogen based cryostat (Hope, 1994; Parkin & Hope, 1998).
Diffraction data were collected with the crystal at 90K, which is standard practice in this laboratory for the majority of flash-cooled crystals.

Geometry. All esds (except the esd in the dihedral angle between two l.s. planes) are estimated using the full covariance matrix. The cell esds are taken into account individually in the estimation of esds in distances, angles and torsion angles; correlations between esds in cell parameters are only used when they are defined by crystal symmetry. An approximate (isotropic) treatment of cell esds is used for estimating esds involving l.s. planes.

Refinement. Refinement progress was checked using *Platon* (Spek, 2009) and by an *R*-tensor (Parkin, 2000). The final model was further checked with the IUCr utility *checkCIF*.

Fractional atomic coordinates and isotropic or equivalent isotropic displacement parameters (Å²)

	x	*y*	*z*	U_{iso}*/U_{eq}
Cl1	0.02919 (8)	0.26975 (5)	0.32981 (6)	0.02188 (17)
N1	0.1115 (3)	0.61456 (15)	0.38285 (18)	0.0172 (5)
N2	−0.0616 (3)	0.59391 (15)	0.23466 (18)	0.0177 (5)
O1	0.6632 (2)	0.62630 (14)	0.70648 (16)	0.0267 (5)
H1O	0.754 (4)	0.658 (2)	0.685 (2)	0.040*
O2	−0.3960 (2)	0.45255 (13)	−0.15434 (15)	0.0246 (5)
H2O	−0.407 (3)	0.386 (2)	−0.155 (2)	0.037*
C1	0.0899 (3)	0.56926 (18)	0.2872 (2)	0.0196 (6)
H1	0.168035	0.527175	0.261384	0.023*
C2	−0.0294 (3)	0.66978 (18)	0.3909 (2)	0.0201 (6)
H2	−0.047100	0.709198	0.450155	0.024*
C3	−0.1369 (3)	0.65700 (19)	0.2986 (2)	0.0209 (6)
H3	−0.244440	0.685964	0.280713	0.025*
C4	0.2593 (3)	0.61151 (18)	0.4634 (2)	0.0170 (6)
C5	0.4107 (3)	0.64043 (18)	0.4386 (2)	0.0187 (6)
H5	0.420025	0.657846	0.367563	0.022*
C6	0.5480 (3)	0.64350 (17)	0.5191 (2)	0.0187 (6)
H6	0.653195	0.661931	0.503157	0.022*
C7	0.5329 (3)	0.61976 (18)	0.6233 (2)	0.0195 (6)
C8	0.3809 (3)	0.58845 (18)	0.6463 (2)	0.0199 (6)
H8	0.371354	0.570419	0.717145	0.024*
C9	0.2436 (3)	0.58362 (18)	0.5658 (2)	0.0204 (6)
H9	0.139637	0.561368	0.580702	0.024*
C10	−0.1400 (3)	0.55635 (18)	0.1320 (2)	0.0173 (6)
C11	−0.1393 (3)	0.45368 (19)	0.1120 (2)	0.0222 (7)
H11	−0.082486	0.408543	0.163846	0.027*
C12	−0.2225 (3)	0.41836 (19)	0.0158 (2)	0.0231 (7)
H12	−0.221456	0.348340	0.000365	0.028*
C13	−0.3082 (3)	0.48456 (19)	−0.0591 (2)	0.0186 (6)
C14	−0.3043 (3)	0.58696 (19)	−0.0383 (2)	0.0204 (6)
H14	−0.359489	0.632414	−0.090377	0.025*
C15	−0.2207 (3)	0.62337 (19)	0.0576 (2)	0.0201 (6)
H15	−0.218569	0.693606	0.072208	0.024*

Atomic displacement parameters (Å²)

	U^{11}	U^{22}	U^{33}	U^{12}	U^{13}	U^{23}
Cl1	0.0211 (3)	0.0216 (3)	0.0222 (4)	0.0002 (3)	0.0016 (3)	0.0014 (3)
N1	0.0161 (12)	0.0175 (11)	0.0171 (13)	0.0012 (9)	0.0003 (10)	−0.001 (1)
N2	0.0184 (13)	0.0184 (11)	0.0155 (13)	0.0004 (9)	0.0008 (10)	−0.0011 (9)
O1	0.0184 (11)	0.0370 (12)	0.0223 (12)	−0.0078 (9)	−0.0031 (9)	0.0074 (9)
O2	0.0334 (12)	0.0194 (10)	0.0176 (12)	−0.0022 (9)	−0.0044 (10)	−0.0014 (9)
C1	0.0202 (15)	0.0199 (14)	0.0180 (17)	0.0023 (11)	0.0015 (13)	0.0003 (12)
C2	0.0191 (15)	0.0226 (14)	0.0197 (17)	0.0058 (11)	0.0062 (13)	−0.0025 (12)
C3	0.0180 (15)	0.0222 (14)	0.0222 (17)	0.0054 (12)	0.0028 (13)	−0.0001 (12)
C4	0.0156 (14)	0.0183 (13)	0.0160 (16)	−0.0002 (11)	0.0000 (12)	−0.0012 (12)
C5	0.0222 (16)	0.0182 (14)	0.0158 (16)	0.0015 (11)	0.0035 (13)	−0.0006 (11)
C6	0.0182 (15)	0.0181 (14)	0.0198 (16)	−0.0012 (11)	0.0035 (13)	0.0017 (12)
C7	0.0200 (15)	0.0185 (13)	0.0179 (16)	0.0007 (11)	−0.0021 (13)	0.0016 (12)
C8	0.0228 (16)	0.0238 (15)	0.0135 (16)	−0.0018 (12)	0.0041 (13)	0.0053 (12)
C9	0.0189 (15)	0.0188 (14)	0.0229 (18)	−0.0018 (11)	0.0022 (13)	0.0006 (12)
C10	0.0161 (15)	0.0196 (14)	0.0155 (16)	−0.0014 (11)	0.0005 (12)	−0.0026 (12)
C11	0.0227 (16)	0.0187 (14)	0.0233 (17)	0.0040 (12)	−0.0015 (13)	0.0030 (12)
C12	0.0280 (17)	0.0178 (14)	0.0225 (18)	−0.0012 (12)	0.0015 (14)	0.0001 (12)
C13	0.0182 (15)	0.0238 (14)	0.0138 (16)	−0.0031 (11)	0.0026 (12)	−0.0021 (12)
C14	0.0258 (16)	0.0188 (14)	0.0163 (16)	0.0027 (12)	0.0027 (13)	0.0022 (12)
C15	0.0235 (16)	0.0177 (14)	0.0185 (16)	0.0000 (11)	0.0017 (13)	−0.0010 (12)

Geometric parameters (Å, º)

N1—C1	1.342 (3)	C5—H5	0.9500
N1—C2	1.384 (3)	C6—C7	1.391 (4)
N1—C4	1.442 (3)	C6—H6	0.9500
N2—C1	1.341 (3)	C7—C8	1.389 (3)
N2—C3	1.385 (3)	C8—C9	1.382 (3)
N2—C10	1.441 (3)	C8—H8	0.9500
O1—C7	1.366 (3)	C9—H9	0.9500
O1—H1O	0.93 (3)	C10—C15	1.380 (3)
O2—C13	1.364 (3)	C10—C11	1.386 (3)
O2—H2O	0.89 (3)	C11—C12	1.376 (4)
C1—H1	0.9500	C11—H11	0.9500
C2—C3	1.350 (4)	C12—C13	1.393 (4)
C2—H2	0.9500	C12—H12	0.9500
C3—H3	0.9500	C13—C14	1.384 (3)
C4—C9	1.383 (4)	C14—C15	1.378 (4)
C4—C5	1.384 (3)	C14—H14	0.9500
C5—C6	1.381 (4)	C15—H15	0.9500
C1—N1—C2	109.0 (2)	O1—C7—C6	122.6 (2)
C1—N1—C4	126.4 (2)	C8—C7—C6	120.1 (3)
C2—N1—C4	124.5 (2)	C9—C8—C7	119.8 (3)
C1—N2—C3	108.7 (2)	C9—C8—H8	120.1

C1—N2—C10	126.4 (2)	C7—C8—H8	120.1
C3—N2—C10	124.7 (2)	C8—C9—C4	119.3 (3)
C7—O1—H1O	110.7 (19)	C8—C9—H9	120.3
C13—O2—H2O	111.0 (19)	C4—C9—H9	120.3
N2—C1—N1	107.9 (2)	C15—C10—C11	121.6 (3)
N2—C1—H1	126.1	C15—C10—N2	118.9 (2)
N1—C1—H1	126.1	C11—C10—N2	119.4 (2)
C3—C2—N1	107.0 (2)	C12—C11—C10	118.7 (2)
C3—C2—H2	126.5	C12—C11—H11	120.6
N1—C2—H2	126.5	C10—C11—H11	120.6
C2—C3—N2	107.4 (2)	C11—C12—C13	120.4 (2)
C2—C3—H3	126.3	C11—C12—H12	119.8
N2—C3—H3	126.3	C13—C12—H12	119.8
C9—C4—C5	121.6 (3)	O2—C13—C14	117.9 (2)
C9—C4—N1	118.3 (2)	O2—C13—C12	122.4 (2)
C5—C4—N1	120.1 (2)	C14—C13—C12	119.7 (3)
C6—C5—C4	118.8 (3)	C15—C14—C13	120.4 (2)
C6—C5—H5	120.6	C15—C14—H14	119.8
C4—C5—H5	120.6	C13—C14—H14	119.8
C5—C6—C7	120.4 (3)	C14—C15—C10	119.1 (2)
C5—C6—H6	119.8	C14—C15—H15	120.5
C7—C6—H6	119.8	C10—C15—H15	120.5
O1—C7—C8	117.4 (3)		

C3—N2—C1—N1	0.4 (3)	C6—C7—C8—C9	−1.8 (4)
C10—N2—C1—N1	−175.5 (2)	C7—C8—C9—C4	−0.9 (4)
C2—N1—C1—N2	−0.3 (3)	C5—C4—C9—C8	2.6 (4)
C4—N1—C1—N2	−177.5 (2)	N1—C4—C9—C8	−174.5 (2)
C1—N1—C2—C3	0.1 (3)	C1—N2—C10—C15	−135.4 (3)
C4—N1—C2—C3	177.3 (2)	C3—N2—C10—C15	49.3 (4)
N1—C2—C3—N2	0.2 (3)	C1—N2—C10—C11	47.6 (4)
C1—N2—C3—C2	−0.4 (3)	C3—N2—C10—C11	−127.8 (3)
C10—N2—C3—C2	175.7 (2)	C15—C10—C11—C12	−0.5 (4)
C1—N1—C4—C9	−127.9 (3)	N2—C10—C11—C12	176.5 (3)
C2—N1—C4—C9	55.3 (3)	C10—C11—C12—C13	−1.2 (4)
C1—N1—C4—C5	55.0 (4)	C11—C12—C13—O2	−178.2 (3)
C2—N1—C4—C5	−121.8 (3)	C11—C12—C13—C14	2.5 (4)
C9—C4—C5—C6	−1.5 (4)	O2—C13—C14—C15	178.5 (3)
N1—C4—C5—C6	175.5 (2)	C12—C13—C14—C15	−2.2 (4)
C4—C5—C6—C7	−1.2 (4)	C13—C14—C15—C10	0.5 (4)
C5—C6—C7—O1	−176.8 (2)	C11—C10—C15—C14	0.9 (4)
C5—C6—C7—C8	2.8 (4)	N2—C10—C15—C14	−176.1 (2)
O1—C7—C8—C9	177.9 (2)		

Hydrogen-bond geometry (Å, º)

D—H···*A*	*D*—H	H···*A*	*D*···*A*	*D*—H···*A*
O1—H1*O*···Cl1^{i}	0.93 (3)	2.06 (3)	2.975 (2)	169 (3)

O2—H2*O*···Cl1^{ii}	0.89 (3)	2.13 (3)	3.0118 (19)	171 (3)
C1—H1···O1^{i}	0.95	2.45	3.280 (3)	145
C1—H1···O2^{iii}	0.95	2.51	3.271 (3)	137
C2—H2···Cl1^{iv}	0.95	2.80	3.647 (3)	150
C3—H3···Cl1^{v}	0.95	2.74	3.655 (3)	163

Symmetry codes: (i) −*x*+1, −*y*+1, −*z*+1; (ii) *x*−1/2, −*y*+1/2, *z*−1/2; (iii) −*x*, −*y*+1, −*z*; (iv) −*x*, −*y*+1, −*z*+1; (v) −*x*−1/2, *y*+1/2, −*z*+1/2.